THE UNIVERSITY of EDINBURGH

Edinburgh Research Explorer

A comparison of the influence of nonlinear and linear creep on the behaviour of FRP-bonded metallic beams at warm temperatures

Citation for published version:
Wang, S, Stratford, T & Reynolds, T 2022, 'A comparison of the influence of nonlinear and linear creep on the behaviour of FRP-bonded metallic beams at warm temperatures', *Composite Structures*, vol. 281, 115117. https://doi.org/10.1016/j.compstruct.2021.115117

Digital Object Identifier (DOI):
10.1016/j.compstruct.2021.115117

Link:
Link to publication record in Edinburgh Research Explorer

Document Version:
Peer reviewed version

Published In:
Composite Structures

General rights
Copyright for the publications made accessible via the Edinburgh Research Explorer is retained by the author(s) and / or other copyright owners and it is a condition of accessing these publications that users recognise and abide by the legal requirements associated with these rights.

Take down policy
The University of Edinburgh has made every reasonable effort to ensure that Edinburgh Research Explorer content complies with UK legislation. If you believe that the public display of this file breaches copyright please contact openaccess@ed.ac.uk providing details, and we will remove access to the work immediately and investigate your claim.

OPEN ACCESS

Download date: 21. Dec. 2022

A comparison of the influence of nonlinear and linear creep on the behaviour of FRP-bonded metallic beams at warm temperatures

S. Wang[1]*, T. Stratford[1] and T.P.S Reynolds[1]
[1]School of Engineering, Institute for Infrastructure and Environment, The University of Edinburgh
The King's Buildings, Mayfield Road, Edinburgh, Scotland, UK, EH9 3FG
Email: songbo.wang@ed.ac.uk, tim.stratford@ed.ac.uk, t.reynolds@ed.ac.uk
* Corresponding Author

Abstract
This study investigates whether it is necessary to consider nonlinear (rather than linear) adhesive viscoelasticity when considering the behaviour of an FRP-bonded metallic beam at warm service temperatures (25°C, 30°C and 40°C). The paper presents finite element analyses that compare the effects of nonlinear and linear creep in the bonded joint for two different FRP-strengthened metallic beams (steel and cast-iron). This modelling work incorporates a viscoelastic adhesive constitutive model determined using a dynamic mechanical analyser for a commonly used ambient cure structural epoxy adhesive. The nonlinear viscoelastic behaviour of the strengthening adhesive was characterised using time-temperature superposition combined with the parallel rheological framework model. The study found that a model incorporating nonlinear viscoelastic creep only leads to a slightly larger joint slip (maximum 1.0% after 1 year) and a slightly lower CFRP axial stress (maximum 2.4% after 1 year), compared to an equivalent model using linear creep. This has a limited impact on the structural performance for the cases studied. In most cases, the simpler linear viscoelastic constitutive model is sufficient to analyse the behaviour of the FRP-bonded metallic beam in a warm environment.

Keywords: FRP-strengthened structures; Ambient-cured adhesive; Nonlinear viscoelastic creep; Differential thermal expansion.

1 Introduction

The strengthening of metallic beams by externally bonding a fibre-reinforced polymer (FRP) plate has become a popular retrofit procedure due to its ease of installation [1–5]. Load transmission from the composite plate to the beam is accomplished using an ambient-cured adhesive joint that does not require elevated-temperature cure. Commonly used ambient-cured epoxy resins have tan δ-peak glass transition temperatures (T_g) around 50°C [3,4,6–8]. The transition of the adhesive from a glassy to a rubbery state results in a significant decrease in its stiffness [7–10], and is accompanied by viscoelasticity and increased creep.

Some recent studies [11–13] have investigated the viscoelastic response of FRP-to-concrete bonded joints; however, less attention has been given to the viscoelastic response of FRP-to-metal joints. The authors previously investigated the influence of *linear* viscoelasticity upon the performance of metallic beams strengthened with CFRP plates [14], by conducting finite element modelling that incorporated a linear viscoelastic constitutive adhesive model. The study found that linear creep of the adhesive resulted in greater slip deformation within the bonded joint with time compared to a pure elastic analysis. This might lead to joint damage and reduce the effectiveness of the FRP-bonded strengthening, potentially resulting in failure within a typical service life [14].

The current paper compares the effects of *nonlinear* and linear viscoelasticity of the adhesive through a finite element study to examine whether it is necessary to consider the nonlinear viscoelastic behaviour in design.

1.1 Nonlinear viscoelasticity for epoxy adhesives

The viscoelastic behaviour resulting from stress is a combination of an instantaneous elastic strain followed by a time-dependent viscous strain. Figure 1 illustrates classic stress-dependent creep curves $\varepsilon(t, \sigma)$ of nonlinear viscoelastic polymers at fixed temperature (T).

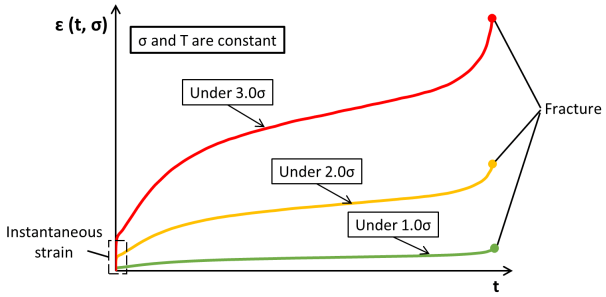

Figure 1: Nonlinear viscoelastic creep under different values of constant stress

For linear creep (as previously examined by the authors [14]), the creep strain is proportion to the applied stress. If the creep strain is not proportion to the applied stress, the creep is nonlinear [15–18]. For nonlinear viscoelasticity, the creep compliance $D(t, \sigma)$ varies with stress level, and can be defined as:

$$D(t,\sigma) = \frac{\varepsilon(t,\sigma)}{\sigma} \quad (1)$$

The stress-dependent nonlinear creep behaviour is likely to result in additional slip deformation due to the large, concentrated stress at the end of the FRP plate, and this will potentially reduce the effectiveness of strengthening more quickly. It is also possible, however, that the increased creep could accelerate the redistribution of the interfacial stress within the bonded joint, which will be beneficial for reducing the concentrated peak stress at the plate end [9,17].

Houhou *et al.* [17] implemented the modified Burgers' model in the finite element system to analyse the effect of adhesive nonlinear creep on FRP to concrete bonded assemblies. It was found that compared to linear creep, nonlinear creep led to a greater reduction in the peak stress at the plate-end and a greater increase in the effective transfer length. A pure elastic analysis (without creep) gave a peak stress of around 16MPa, whereas this was reduced to 9MPa by considering a linear creep model, and 4MPa by considering nonlinear creep. The effective transfer length increased from 72mm (elastic) to 80mm (linear creep), and 81.6mm (nonlinear creep). They did not, however, consider how warm temperatures can bring about greater creep deformation, nor did they consider the impact on the behaviour upon an actual FRP-bonded beam. In addition, the behaviour of concrete and metallic substrates will be different. In FRP-to-concrete joints, the strength of the bonded joint may be limited by the strength of the concrete, but in FRP-to-metal joints the strength of the joint is normally not dependent on the metal, and greater stresses can consequently occur in FRP-to metal adhesive joints that can result in greater creep deformation [1]. The significance of adhesive nonlinear viscoelasticity upon the performance of FRP-bonded metallic beams therefore requires further study.

1.2 Outline of the research presented in this paper

The aims of this study are to explore the influence of nonlinear viscoelastic behaviour of the strengthening adhesive on the long-term behaviour of CFRP-strengthened metallic beams, whether nonlinear viscoelastic creep will bring more severe structural issues than linear viscoelastic creep, and whether it is necessary to consider the nonlinear response (or not) in civil engineering projects. The "warm" temperatures of interest in this study are the elevated temperatures typically experienced during a typical service life, and not the extreme temperatures associated with a fire.

Constant elevated temperatures and constant sustained loads are examined in this study as a means to establish the above objective; however, it should be recognised that real civil engineering structures are subject to both temperatures and loads that are vary with time. This is outside the scope of the current paper, but an analysis of cyclic loading and cyclic temperature effects is being undertaken as part of a follow-up research.

The study has been conducted using finite element (FE) analytical work, using an adhesive constitutive model obtained through testing. The experimental characterisation work of an epoxy resin for FRP bonding was necessary to provide a nonlinear viscoelastic model that was sufficient to use in the FE analyses, so as to contrast the effect of linear and nonlinear adhesive creep upon FRP-strengthened beams. Establishing a comprehensive nonlinear viscoelastic material adhesive model was not, however, the focus of this study.

2 Characterisation of Nonlinear Viscoelastic Adhesive Response

The nonlinear viscoelasticity of the examined adhesive was characterised using a dynamic mechanical analyser (DMA). A parallel rheological framework (PRF) constitutive model was used to describe the adhesive behaviour [19,20], after applying the time-temperature superposition principle (TTSP) to develop

master curves based up on the experimental outcome [17,21]. The fundamental theory is outlined in this section, but more detailed descriptions can be found in the cited references.

2.1 Parallel Rheological Framework model

Linear viscoelasticity of the adhesive layer can be described using a Prony series, and this approach was used in the authors' previous study [14]. The Prony series function, however, is independent of stress or strain, and it is not suitable for representing *nonlinear* viscoelasticity. This study therefore uses the Parallel Rheological Framework (PRF) constitutive model developed by Hurtado *et al.* [22] and implemented in the Abaqus finite element software. The PRF model represents the nonlinear viscoelastic response as a pure elastic link (N_0) and a group of viscoelastic links (N_1 - N_n), as illustrated in Figure 2 [19,20,22,23].

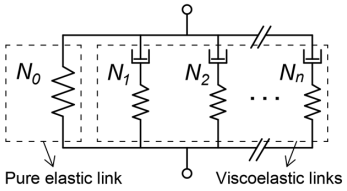

Figure 2: Parallel Rheological Framework (PRF) model concept

The *Yeoh* hyperelastic model [Eq. (2)] is used to specify the elastic part of the response for all the networks (N_0 - N_n), scaled by a stiffness ratio ($SRatio_n$) specific to each network [19,20,22,23]:

$$U = \sum_{i=1}^{3} C_{i0}\,(\bar{I}_1 - 3)^i + \sum_{i=1}^{3} \frac{1}{D_i}(J^{el} - 1)^{2i} \tag{2}$$

where U is the strain energy per unit of reference volume, J^{el} is the elastic volume ratio, C_{i0} and D_i are material parameters, $\bar{I}_1$ is the first deviatoric strain invariant defined as [23,24]:

$$\bar{I}_1 = \bar{\lambda}_1^2 + \bar{\lambda}_2^2 + \bar{\lambda}_3^2 \tag{3}$$

where stretch ratios $\bar{\lambda}_i$ are the ratio of the deformed length l_i to the undeformed length L_i in different directions. Abaqus can calculate the total stress response based on the strain energy, U. The initial shear modulus and bulk modulus are given by [23,24]:

$$G_0 = 2C_{10} \tag{4}$$

$$K_0 = \frac{2}{D_1} \tag{5}$$

Viscous behavior must be defined for each viscoelastic network (N_1 - N_n). It is modelled by assuming the multiplicative split of the deformation gradient ($\mathbf{F}$) and the existence of the creep potential (G^{cr}) [22,23]:

$$\mathbf{F} = \mathbf{F}^e \cdot \mathbf{F}^{cr} \tag{6}$$

$$\dot{\mathbf{F}}^{cr} = \mathbf{F}^{e^{-1}} \cdot \mathbf{D}^{cr} \cdot \mathbf{F}^e \cdot \mathbf{F}^{cr} \tag{7}$$

where $\mathbf{F}^e$ is the elastic part of the deformation gradient, $\mathbf{F}^{cr}$ is the creep part of the deformation gradient in the viscoelastic networks. The creep part of the deformation rate tensor ($\mathbf{D}^{cr}$) in the current configuration is derived from a creep potential ($G^{cr} = G^{cr}(\tau)$) using the flow rule [22,23]:

$$\mathbf{D}^{cr} = \dot{\lambda}\frac{\partial G^{cr}(\boldsymbol{\tau})}{\partial \tau} \tag{8}$$

where τ is the Kirchhoff stress, $\dot{\lambda}$ is the proportionality factor. In this model, the creep potential is given by the effective Kirchoff stress, $G^{cr}(\tau) = q$, and the proportionality factor is taken as $\dot{\lambda} = \dot{\bar{\varepsilon}}^{cr}$, where $\dot{\bar{\varepsilon}}^{cr}$ is the equivalent creep stain rate. Followed by calculation and simplification, the flow rule can be written as [22,23]:

$$\mathbf{D}^{cr} = \frac{3}{2q}\dot{\bar{\varepsilon}}^{cr}\bar{\boldsymbol{\tau}} \tag{9}$$

In this study, the Abaqus built-in *power-law strain hardening* model is applied to determine the equivalent creep stain rate [19,20,23]:

$$\dot{\bar{\varepsilon}}^{cr} = (A\tilde{q}^n[(m+1)\bar{\varepsilon}^{cr}]^m)^{\frac{1}{m+1}} \tag{10}$$

where $\bar{\varepsilon}^{cr}$ is the equivalent creep strain, $\tilde{q}$ is the equivalent deviatoric Kirchhoff stress, A, n and m are material parameters. Note that the case $m = 0$ and $n = 1$ represents linear viscoelasticity.

In section 4, the obtained parameters of Eq. (2) and Eq. (10) from the DMA characterising test described in section 3 are used as an input to the Abaqus FE model.

2.2 Time - temperature superposition

Time – temperatures superposition principle (TTSP) was used in this study to build multiple master curves, each at a different level of strain, from the DMA test described in Section 3. The applied shift factors (α_T) described as in [Eq. (11)] are calculated using the Williams-Landel-Ferry (WLF) equation [Eq. (12)] [17,25,26]:

$$log(\alpha_T) = log\left(\frac{\omega'}{\omega}\right) \tag{11}$$

$$log(\alpha_T) = \frac{-C_1(T - T_{ref})}{C_2 + (T - T_{ref})} \tag{12}$$

where ω is the applied frequency during the accelerated test, ω' is the shifted frequency, T is the applied temperature during the accelerated test, T_{ref} is the reference temperature. C_1 and C_2 are material parameters.

The next section of the paper describes the PRF and WLF parameters that were established for the bonding adhesive studied in this paper.

3 Experimental characterisation of the epoxy adhesive

The adhesive characterised in this study was an epoxy resin commonly used to rehabilitate civil engineering structures, Sikadur-330 [27]. Dynamic Mechanical Analysis (DMA) was used to characterise the adhesive, using a DMA 8000 [28].

Combining the DMA test with TTSP is a convenient accelerated method for estimating the long-term viscoelastic characteristics of materials using a short test period. The adhesive model established here was intended to be sufficient. Far longer timescales (several decades) are of importance for externally bonded FRP strengthening, but establishing a comprehensive nonlinear adhesive model based on real-time long-term tests was not possible within the scope of the current study. This would likely require a traditional sustained load creep test in which sustained stress is applied to adhesive specimens over a long timescale, rather than a DMA test on small samples over timescales of hours, something that was not possible within the current project and that would require separate research. [13,17,21].

3.1 Adhesive characterisation method

The used specimens and experiments were conducted according to ISO 6721 [29]. The two-part epoxy was mixed based on the manufacturer's datasheet [27] and cast into rectangular samples, nominally 45 × 10 × 1.7mm [29].

The samples were cured for seven days at 21°C prior to DMA testing, resulting in an onset T_g of 38.0°C and a peak tan δ T_g of 49.0°C [14]. Whilst the current conditions (temperature and duration) have an impact on the properties of adhesives, this has been examined elsewhere [7,8,30]. For the purposes of this study, a single cure condition of seven days cure was selected as typical for large FRP-bonded civil engineering structures [9]. The degree of cure and the glass transition temperature of the adhesive would be lower for a structure that is required to re-enter service earlier than 7 days or is cured at a lower temperature.

Dynamic Mechanical Analysis (DMA) applies a sinusoidal oscillating force or displacement to determine the change in modulus of the tested sample, in terms of both the amplitude of the deformation at the peak of the sine wave and the lag between the stress and strain waves [25]. In this study a series of multi-frequency scans were conducted.

A dual cantilever configuration was used to ensure that the specimen remained stable and received a relatively uniform strain under larger displacement levels [25]. Under isothermal conditions (from 25°C to 100°C with a variation of 5°C between two scan steps), multi-frequency scans were performed on the adhesive (at 21 frequencies: 0.010, 0.016, 0.025, 0.040, 0.063, 0.100, 0.158, 0.251, 0.398, 0.631, 1.000, 1.585, 2.512, 3.981, 6.310, 10.000, 15.849, 25.119, 39.811, 63.096, and 100.000 (Hz)). The DMA automatically scanned multiple times at different frequency levels during each scan step and outputted the average experimental results [17,25]. The DMA multi-frequency scans test was performed for each adhesive sample with a selected displacement amplitude, resulting in a total of three experiments (using three samples) with three different displacement amplitudes (0.005mm, 0.020mm, and 0.040mm) to allow the nonlinear constitutive response to be determined.

For the test under each displacement amplitude, the storage modulus was measured at each scanning step, and the corresponding master curve was established by applying TTSP. The PRF constitutive model could then be developed based on the three master curves obtained with different displacement (strain) levels.

3.2 Adhesive characterisation results

The adhesive's thermal-viscoelastic responses under different applied displacement (strain) amplitudes are shown in Figure 3 (a-c), which show the experimentally-obtained storage modulus variation with frequency at different temperatures. TTSP was employed to build the modulus master curves for a reference temperature of T_{ref} = 40°C, (which is where the glass transition process starts to occur and the modulus starts to reduce significantly).

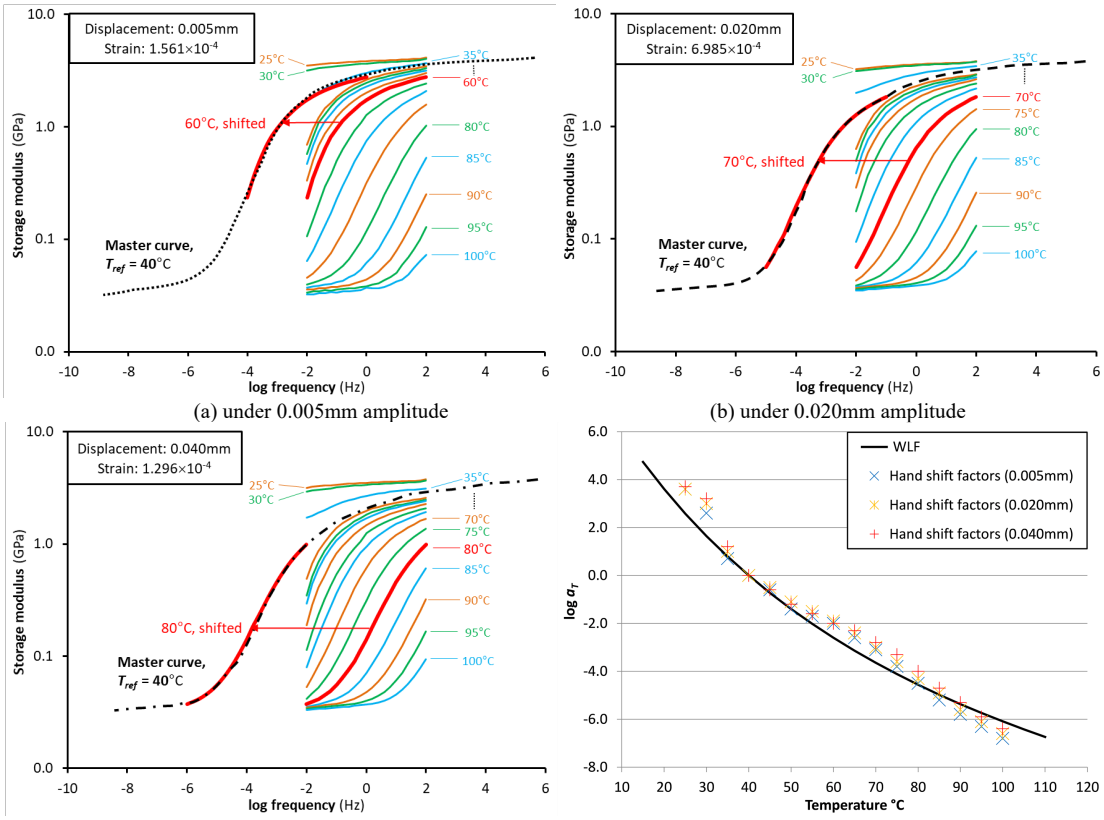

(a) under 0.005mm amplitude (b) under 0.020mm amplitude

(c) under 0.040mm amplitude (d) for corresponding three master curves

Figure 3: (a - c) Storage modulus master curves for T_{ref} = 40°C and the raw storage modulus data at three different strain levels; (d) the manual shift factors fitted to WLF

3.3 Nonlinear viscoelastic constitutive model

The manual shift factors illustrated in Figure 3 (d) were fitted to the WLF law [Eq. (12)] to determine the material parameters, C_1 = 18.567 and C_2 = 122.99 (°C). The master curves were fitted using a PRF model including a *Yeoh* function [Eq. (2)] and a three-term *power-law strain hardening* function [Eq. (10)]. These resulted in the master curves shown in Figure 4, and described by the parameters given in Table 1. The *Yeoh* function in the PRF model captures the instantaneous hyperelastic behaviour; however, as this study focuses on the time-dependent creep behaviour, it is assumed that the adhesive exhibits instantaneous pure elastic behaviour, so only two parameters (C_{10} and D_1) were used to describe the adhesive's instantaneous elastic response. The selected number of significant digits is to ensure the accuracy of the constitutive model.

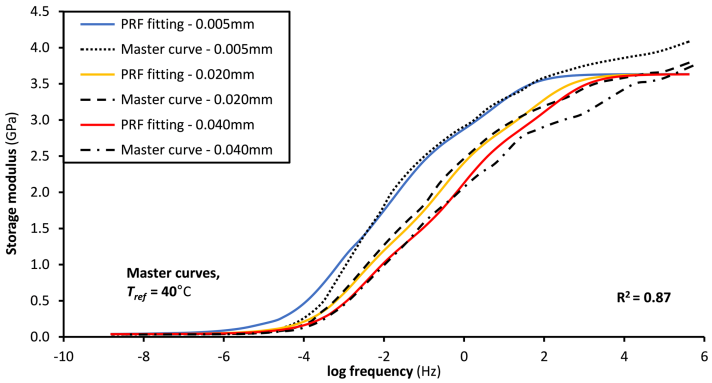

Figure 4: Master curves for T_{ref} = 40°C and the corresponding PRF model fitting

Table 1: Parameters in the adhesive PRF model

C_{10} (MPa)	C_{20} (MPa)	C_{30} (MPa)	D_1 (MPa^{-1})	D_2 (MPa^{-1})	D_3 (MPa^{-1})
Yeoh parameters					
758.453	0	0	0.001	0	0

SRatio (-)	A (MPa^{-n}s$^{-(m+1)}$)	n (-)	m (-)	T_{ref} (°C)	C_1 (-)	C_2 (°C)
Power-law strain hardening parameters				WLF parameters		
0.4287	8.744×10^{-04}	2.399	-0.1490	40	18.567	122.99
0.3116	2.466×10^{-01}	2.341	-0.1135	40	18.567	122.99
0.2515	2.674×10^{-05}	1.710	-0.1780	40	18.567	122.99

Figure 5 shows the creep compliance of the examined structural adhesive under different levels of stress and temperature.

Note that the PRF model fitting becomes less accurate in the high-frequency range (> 10^0Hz) of the master curves (Figure 4) due to the limited number of terms of the *Power-law strain hardening* parameters used by the curve fitting tool. However, this only affects the accuracy of the extremely short-term viscoelastic creep response (< 10^3s), which is not shown in Figure 5. The fitting is also less accurate around the 10^4Hz range due to the rapid change of the storage modulus, which could cause the creep compliance curves (Figure 5) to show relatively larger nonlinearity in the region where the slope decreases rapidly. A more advanced nonlinear material model would be preferable; nevertheless, the material model developed in this section is sufficient for accomplishing the task of this paper, which is to investigate the implications of nonlinear viscoelastic creep behaviour of the adhesive joint on a CFRP-bonded metallic beam. More comprehensive material characterisation work would be an individual project and is out of the scope of this study.

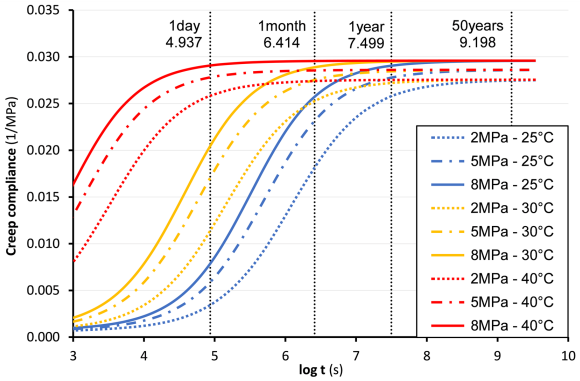

Figure 5: Creep compliance curves obtained for different temperatures (25°C, 30°C and 40°C) and stresses (2MPa, 5MPa and 8MPa)

Creep compliance curves for different temperature levels can be obtained by shifting the referenced (40°C) curves along the horizontal axis using TTSP. However, these timescales are at the edge of the available data for higher temperature levels (> 40°C). For the temperature of 50°C as an example, the adhesive response can be only predicted up to 1 year using the available data (applying a shift factor of $\log(\alpha_{50}) = -1.396$, obtained from the WLF equation [Eq. (2)]).

4 Numerical modelling

4.1 Models for two FRP-bonded metallic beams

This paper examines the same two benchmark beams examined in Wang *et al.* [14] (where linear creep was considered):

- an FRP-bonded steel beam, shown in Figure 6 (a);
- an FRP-bonded cast-iron beam, shown in Figure 6 (b).

The lab-scale FRP-bonded steel I-beam is similar to the I-beam tested by Stratford and Bisby [9]. The applied load of 110kN results in first yield of the steel, and whilst this load is larger than the serviceability limit state, it was applied to allow creep effects to be studied. The real-scale FRP-bonded cast-iron I-beam is similar to the beam examined by Stratford and Cadei [31] and is based on historic rail bridges described in Cadei *et al*. [1]. The applied 40kN/m uniform load corresponds to the ultimate limit state of a real design [1].

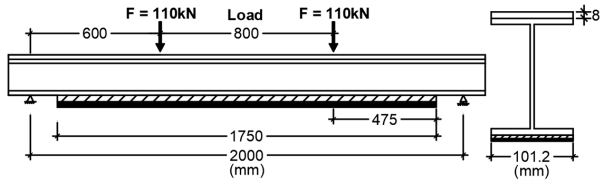

(a) CFRP-strengthened steel beam

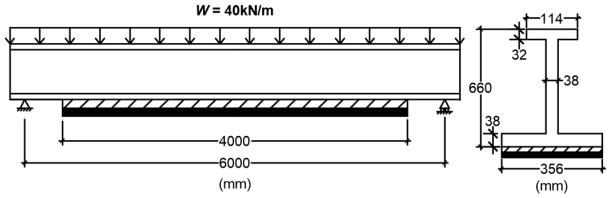

(b) CFRP-strengthened cast-iron beam

Figure 6: Two metallic beams externally strengthened using CFRP plate

3D finite element analysis was used to compare the effects of nonlinear viscoelastic creep and linear viscoelastic creep on the CFRP-bonded beams, and hence discuss whether it is necessary to model nonlinear creep behaviour in design. 3D models were necessary to allow nonlinear viscoelasticity to be studied, which differ from the 2D models used in the previous study [14].

Table 2 summaries the material properties of each component of the model. For the strengthened steel beam, the steel I-beam was modelled as an isotropic elastoplastic material with a yield strength of σ_{sy} = 355MPa; while the FRP plate was modelled as an orthotropic elastic material with an elastic modulus of E_{ss3} = 170GPa in the direction of the fibres.

The strengthened cast-iron I-beam model was constructed using a similar method, but the material properties of the beam and the applied CFRP plate were different. The cast-iron was modelled as an isotropic elastic material with a maximum permissible tensile stress of σ_{ct} = 14.4MPa. To effectively strengthen the 6.0m span cast-iron beam, a thicker (t_{cs} = 11mm) and stiffer CFRP plate (E_{cs3} = 360GPa) was applied.

Table 2: Material properties of the two beams

Components		Strengthened steel beam (s)	Strengthened cast-iron beam (c)
Beam (b)	Type	Steel, UKB (178×102×19)	Cast-iron
	Young's modulus	E_{sb} = 205GPa;	E_{cb} = 138GPa;
	Poisson's ratio	μ_{sb} = 0.3;	μ_{cb} = 0.3;
	Maximum permissible tensile stress	σ_{sy} = 355MPa;	σ_{ct} = 14.4MPa;
	Coefficients of thermal expansion	$\alpha_{sb} = 1.1\times10^{-05}$/°C	$\alpha_{cb} = 1.1\times10^{-05}$/°C
Strengthening (s)	Elastic modulus in three directions	E_{ss3} = 170GPa,	E_{cs3} = 360GPa,
		$E_{ss1} = E_{ss2}$ = 7.44GPa;	$E_{cs1} = E_{cs2}$ = 10GPa;
	Shear modulus in three directions	G_{ss12} = 2.6GPa,	G_{cs12} = 3.7GPa,
		$G_{ss13} = G_{ss23}$ = 4.31GPa;	$G_{cs13} = G_{cs23}$ = 26.5GPa;
	Poisson's ratio in three directions	μ_{ss12} = 0.45,	μ_{cs12} = 0.3,
		$\mu_{ss13} = \mu_{ss23}$ = 0.015;	$\mu_{cs13} = \mu_{cs23}$ = 0.0058;
	Coefficients of thermal expansion	$\alpha_{ss33} = 6\times10^{-07}$/°C,	$\alpha_{cs33} = 1\times10^{-06}$/°C,
	in three directions	$\alpha_{ss11} = \alpha_{ss22} = 2.5\times10^{-05}$/°C;	$\alpha_{cs11} = \alpha_{cs22} = 2.8\times10^{-05}$/°C;
	Thickness of the strengthening plate	t_{ss} = 1.4mm	t_{cs} = 11mm
Nonlinear viscoelastic adhesive (a)	Type	PRF model (Table 1);	PRF model (Table 1);
	Coefficients of thermal expansion	$\alpha_a = 4.5\times10^{-05}$/°C;	$\alpha_a = 4.5\times10^{-05}$/°C;
	Thickness of the adhesive layer	t_a = 2mm	t_a = 2mm
Linear viscoelastic adhesive (a)	Type	Prony series ([14]);	Prony series ([14]);
	Coefficients of thermal expansion	$\alpha_a = 4.5\times10^{-05}$/°C;	$\alpha_a = 4.5\times10^{-05}$/°C;
	Thickness of the adhesive layer	t_a = 2mm	t_a = 2mm

The time-dependent behaviour of the two CFRP-strengthened I-beams were subjected to a sustained external load (see Figure 6) and uniform temperature of either:

- 25°C, which is slightly higher than the ambient temperature;
- 30°C, being a typical indicative structural temperature under solar heating in Scotland [32];
- 40°C, which is the reference temperature of the constitutive model (Figure 4), as well as a design temperature for some structures [33].

As noted above, the glass transition temperature of the adhesive depends upon the curing temperature. The temperatures selected for study therefore need to be seen relative to the cure temperature (of 21°C) and the glass transition temperature (peak tan δ T_g = 49°C) of the adhesive. The temperatures selected here are representative of the structural temperature of metallic bridges in Scotland [32,33]. A temperature of 40°C (for 50 years) is intended to be the most critical case for studying the effect of creep, although such a sustained temperature if of course an extreme case. Current design guidelines recommend that the operating temperature of the FRP-strengthened structure should be at least 15°C lower than the peak tan δ T_g of the applied adhesive [1,3,4], which gives a maximum operating temperature of 49°C – 15°C = 34°C.

A higher ambient temperature makes the adhesive more likely to exhibit creep, but can also enhance cure and the T_g of the adhesive [30]. The current study can therefore also be valuable for higher (or lower) temperature conditions, in other regions.

Differential thermal expansion (DTE) can cause significant interfacial stresses within the bonded joint [1,31], because the coefficients of thermal expansion (α) differ greatly between the metallic substrate and bonded composite. The results are presented here with and without DTE effects to highlight this effect.

4.2 Modelling the adhesively bonded joint

Two constitutive models were used for the adhesive to allow the effects of linear and nonlinear viscoelasticity to be contrasted:

- the linear viscoelastic model determined in Wang *et al.* [14] (for the same adhesive as used in the current study); and
- the nonlinear viscoelastic model described in the previous sections and given in Table 1.

The creep behaviour of the adhesive may limit the load transfer ability of the adhesively bonded joint, and the excessive creep deformation may lead to a debonding failure [1]; however, neither the nonlinear constitutive model nor the linear constitutive model can be used to describe the failure of the bonded joint. Therefore, a cohesive zone model (CZM) is used describe the evolution of joint damage that may eventually lead to debonding, by adding a single layer of cohesive elements (t_{coh} = 0.01mm) between the soffit of the I-beam and the adhesive part, as shown in Figure 7.

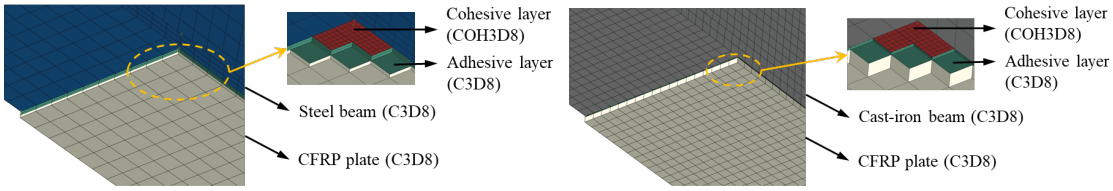

(a) CFRP-strengthened steel beam (b) CFRP-strengthened cast-iron beam

Figure 7: Mesh details of the plate-end

The CZM is from Zhou *et al.* [34], who conducted lap-shear tests on CFRP-to-steel bonded joints to determine their temperature-dependent traction-separation behaviour. The tests showed a bilinear behaviour, and they therefore used a bilinear *Mode II* traction-separation law to model the joint damage. This bilinear law has been adopted in this study and is the same as used in Wang *et al.* [14]. It is shown in Figure 8, where $\tau(\delta)$ is the constitutive relationship between the interfacial shear stress (τ) and *Mode II* separation (δ) [5,34–36]:

$$\tau(\delta) = (1 - D_\delta) K_e \delta \tag{13}$$

K_e is the bond stiffness and D_δ is the damage variable defined as [34–36]:

$$D_\delta = \begin{cases} 0 & \delta \le \delta_0 \quad Elastic\ phase \\ \dfrac{\delta_{max}(\delta - \delta_0)}{\delta(\delta_{max} - \delta_0)} & \delta_0 < \delta < \delta_{max} \quad Softening\ phase \\ 1 & \delta_{max} \le \delta \quad Debonding\ phase \end{cases} \tag{14}$$

where δ_{max} and δ_0 are the separation value corresponding to the maximum shear stress (τ_f) and full failure respectively.

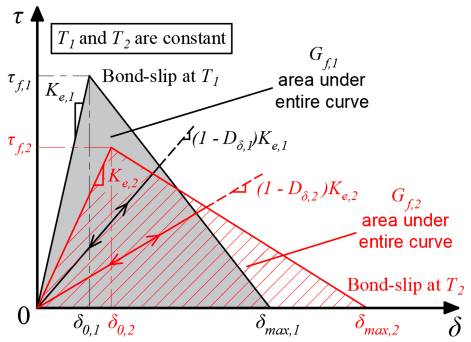

Figure 8: The temperature-dependent damage parameter evolution

The temperature-dependent parameters were obtained by Zhou *et al.*[34] from tests. The temperature-dependent interfacial shear stress (τ_f) and fracture energy (G_f) can be obtained by [34]:

$$\tau_f = -0.2428\,T + 21.141\ (\mathrm{N/mm^2}) \tag{15}$$

$$G_f = -0.00206\,T^2 + 0.1978\,T - 2.6185\ (\mathrm{N/mm}) \tag{16}$$

The temperature-dependent bond stiffness ($K_{e,t}$) obtained in Zhou *et al.*[34] has been modified in this study to allow to be applied over 80°C and to incorporate the time-dependent viscoelastic stiffness of the adhesive using the WLF equation [14]:

$$K_{e,t} = \begin{cases} 1785 \times e^{-0.047 T_t} & 20°\mathrm{C} \le T_t \le 80°\mathrm{C} \\ 98.04 \times e^{-0.011 T_t} & 80°\mathrm{C} < T_t \end{cases} \tag{17}$$

$$-log(t) + log(\alpha_T) = \frac{-C_1(T_t - T_{ref})}{C_2 + (T_t - T_{ref})} \tag{18}$$

where t is the time in seconds, α_t is the shift factor, T_t is the shifted temperature. T_{ref} = 40°C, C_1 = 21.022 and C_2 = 152.64°C were obtained by Wang *et al.* [14] based on charactering the linear viscoelasticity of the same epoxy adhesive.

A strengthened beam should normally be designed so that damage does not occur in the bonded joint in the serviceability limit state (SLS), as damage can reduce the shear strength of the adhesive (see Figure 8) and limit the effectiveness of strengthening [14]. Damage propagation leading to debonding failure is an ultimate limit state, and as mentioned above, both of the beams examined here are subjected to ULS loads to allow the effect of joint damage to be studied.

5 The influence of nonlinear creep on the lab-scale FRP-bonded Steel Beam

The effect of nonlinear creep of the adhesive upon the behaviour of the FRP-bonded steel structure (Figure 6 (a)) is examined in this section. The linear and nonlinear viscoelastic effects are compared to indicate whether it is necessary to consider nonlinear viscoelasticity in design.

Two analyses are provided separately for comparison purposes:

- without differential thermal expansion (DTE);
- with DTE by assuming the structure was strengthened at 25°C.

5.1 Adhesive viscoelasticity, but no differential thermal expansion

Figure 9 illustrates the distribution of slip deformation between the FRP and the bottom flange of the structure at various sustained temperatures for different time period. Figure 10 plots the CFRP axial stress, with a zoom-in view showing the stress in the centre of the beam. The "No Creep" results shown in the plots are a benchmark elastic FE analysis, as currently adopted in design guidelines [1,2]. These are slip and stresses expected to develop in the strengthening system at the ultimate limit state (ULS), as the lab-scale FRP-bonded steel beam bears the maximum load to study the creep effect.

The slight difference between the linear and nonlinear results in the benchmark case (no creep) is due to the fact that the instantaneous elasticity of the adhesive is defined by an instantaneous elastic modulus in the linear model [14], whereas the nonlinear model uses the *Yeoh* hyperelastic law [Eq. (2)] (part of the PRF model shown in Table 1).

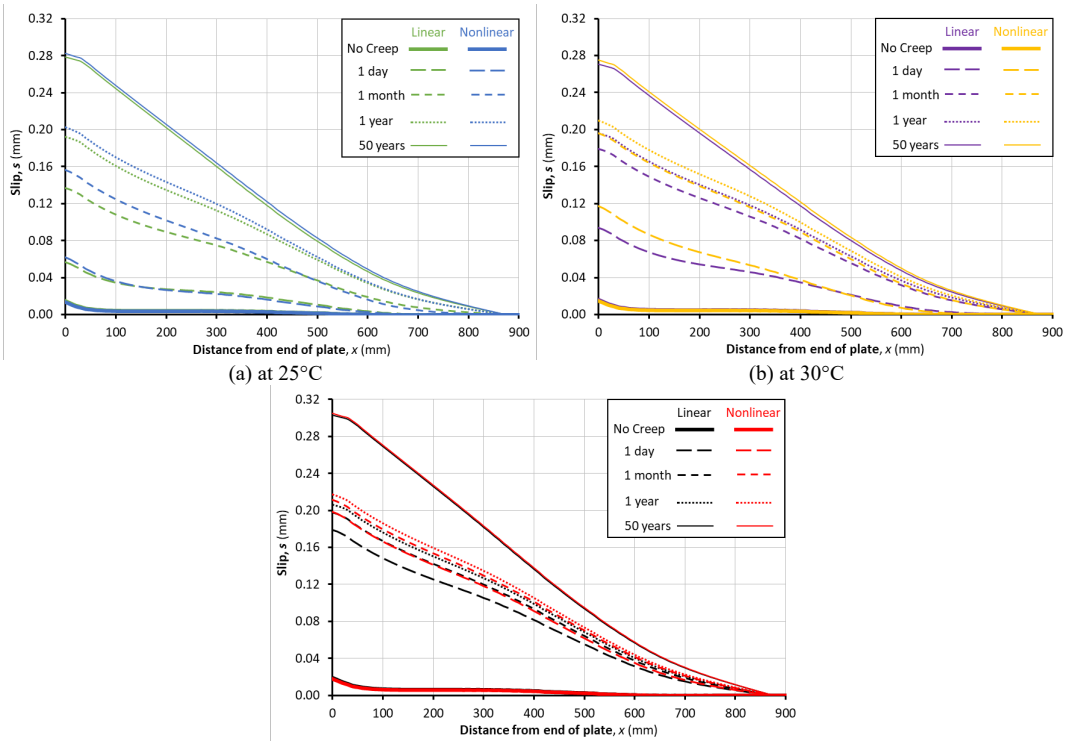

(a) at 25°C (b) at 30°C

(c) at 40°C

Figure 9: Distribution of joint slip, *s* (mm) along the strengthened steel beam with time (without DTE)

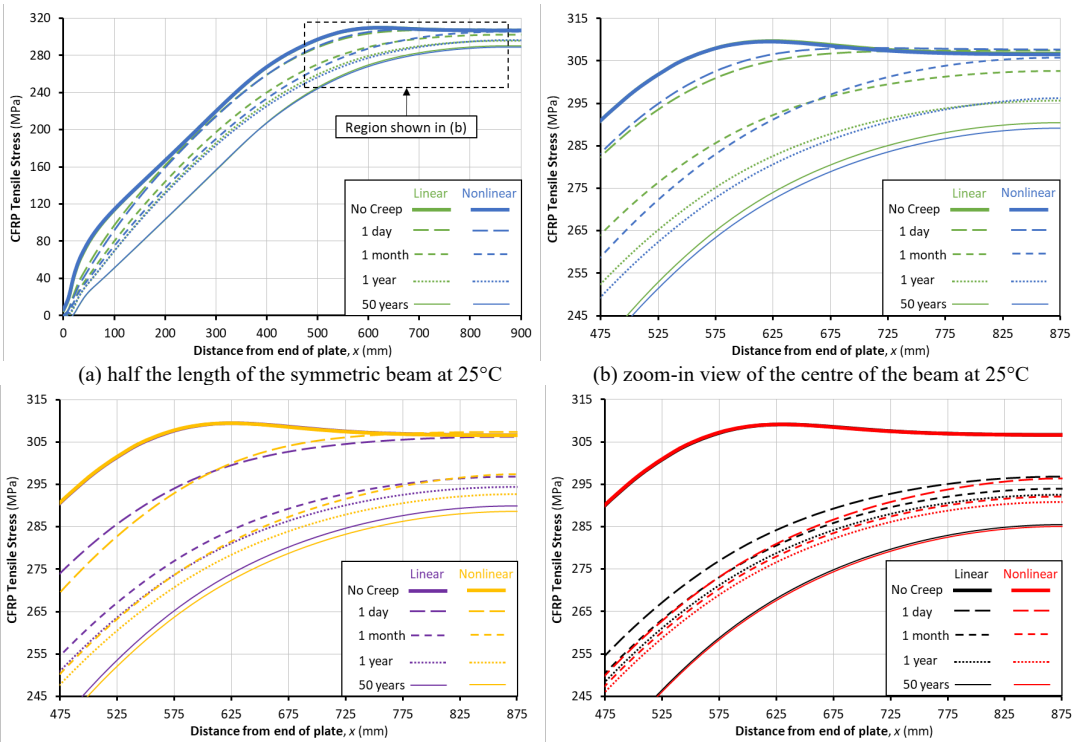

(a) half the length of the symmetric beam at 25°C

(b) zoom-in view of the centre of the beam at 25°C

(c) zoom-in view of the centre of the beam at 30°C

(d) zoom-in view of the centre of the beam at 40°C

Figure 10: Distribution of FRP tensile stress along the strengthened steel structure with time (without DTE)

Introducing nonlinear (compared to linear) viscoelasticity into the adhesive model leads to a greater increase in the slip deformation (maximum 0.022 mm at the plate-end), accompanied by a slightly greater decrease in the CFRP axial stress (maximum 1.85 MPa at the middle of the beam).

- After 1 day to 1 year, the plate-end slip predicted by the nonlinear model is larger than that predicted by the linear model. For example, after 1 year at 25°C, the maximum slip in the nonlinear model is around 0.20mm which is about 0.01mm larger than that in the linear model. 0.01mm would usually be seem negligible in civil engineering structures, but this slip results in a 3.0MPa greater reduction in the FRP axial stress at the loading point (x = 475mm) and consequently results in a reduction in the effectiveness of strengthening that may be significant in design.
- However, at the middle of the beam (x = 875mm), the stress-dependent nonlinear creep does not lead to an obvious larger slip, due to the relatively low stresses in the adhesively bonded joint compared to that at the end of the strengthening plate. The change in CFRP stress is minimal in that area. For designers, this could be seen as beneficial as it maintains the beam's moment capacity at warm temperatures.
- After 50 years, the difference between the plate-end slip caused by nonlinear creep and linear creep is less than 0.4% at all three temperature levels, which results in similar distribution of FRP tensile stress. This suggests that, whilst considering the effect of nonlinear viscoelastic creep is important for timescales up to 1 year (for this scenario), the simpler linear viscoelastic model is probably sufficient for predicting the long-term behaviour of the FRP-bonded steel structure, such as that after 50 years.

Figure 11 shows the damage variable (D_δ) along the bonded joint. For all three examined temperature levels, joint damage has occurred one month after load application, in both the nonlinear and linear models. The nonlinear viscoelasticity does not increase the bonded joint damage, due to the quicker stress distribution behaviour reducing the peak adhesive shear stress. As noted above, the load applied to the lab scale represents the ultimate limit state, and consequently damage of the adhesive joint is to be expected. Damage should be avoided at the serviceability limit state, as it could bring a larger slip deformation, and limit the effectiveness of FRP-bonding.

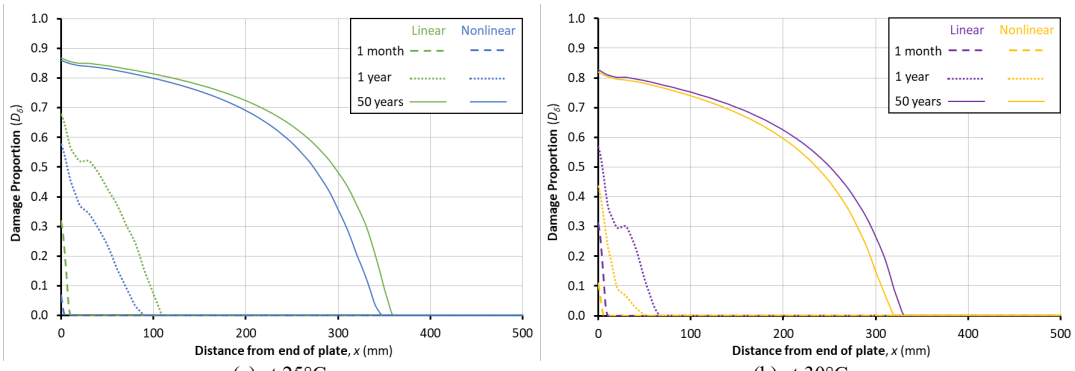

(a) at 25°C (b) at 30°C

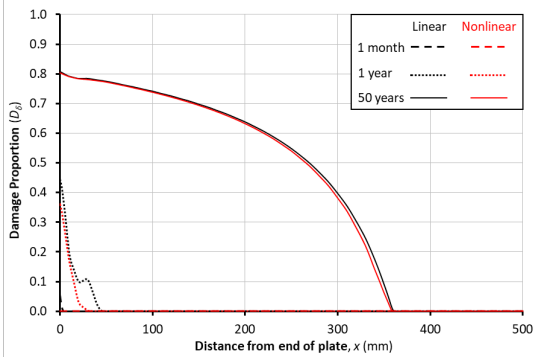

(c) at 40°C

Figure 11: Joint damage proportion (D_δ) growth in the strengthened steel beam (without DTE)

5.2 Adding differential thermal expansion (DTE)

In this section, the effect of DTE is included in the strengthened beam model, assuming that the bonding was applied to the beam at T_{ref} = 25°C. Figure 12 plots the slip, Figure 13 plots the CFRP tensile stress, and Figure 14 shows the damage parameter. The plots at 25°C (when no DTE occurs) are not shown because they are the same as those plotted in the previous section (Figure 9, Figure 10 and Figure 11). The "no creep" results are the benchmark elastic outcome due to the effect of DTE, with an instantaneous maximum shear stress increases of about 4.5MPa at 40°C including DTE.

Including nonlinear viscoelasticity of the adhesive in the FE analyses does not result in a higher joint damage proportion, as shown in Figure 14 (and as also seen in the previous section without DTE). Considering nonlinear viscoelastic behaviour only leads to moderately larger slip and lower CFRP tensile stress before the 1-year period compared to a linear model. The effect of the differential thermal expansion is far larger than the difference between the results from the nonlinear and linear viscoelastic creep models at warm services temperatures.

Whilst DTE results in higher slip (comparing Figure 12 to Figure 9), it appears to be beneficial by maintaining the stress in the strengthening FRP plate during long-term service (comparing Figure 13 to Figure 10, noting the different vertical scales). When the environmental temperature decreases, however, the FRP tensile stress will decrease instantaneously as the DTE is a time-independent effect, which could bring a higher moment to be carried by the metallic beam. The proportion of the irreversible bonded joint damage could be larger under temperature cycles. A study on the impact of cyclic temperature is out of the scope of this article but will be presented in a future paper.

Figure 15 compares the effects of nonlinear and linear creep on the plate-end slip increases with time with and without including DTE.

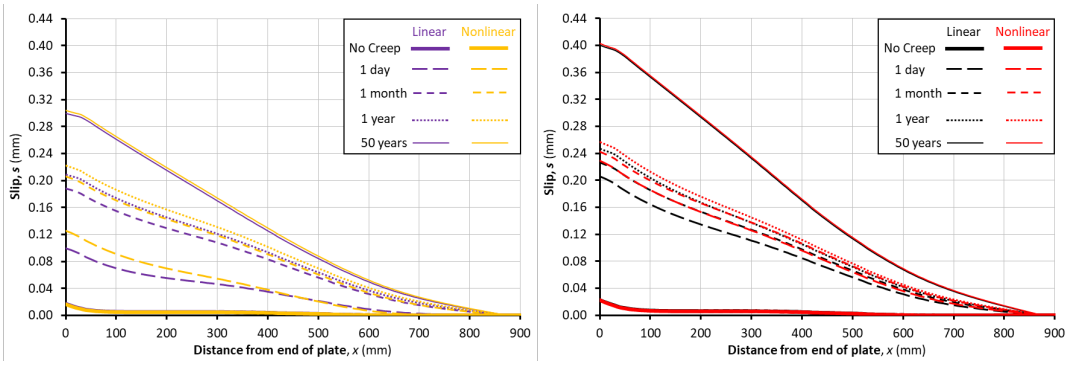

(a) at 30°C (b) at 40°C

Figure 12: Distribution of joint slip, s (mm) of the strengthened steel beam with time (with DTE)

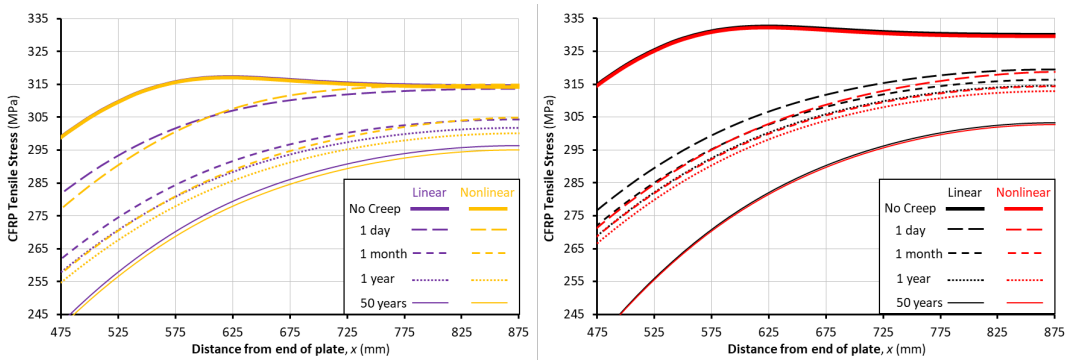

(a) zoom-in view of the centre of the beam at 30°C (b) zoom-in view of the centre of the beam at 40°C

Figure 13: Distribution of FRP tensile stress of the strengthened steel structure with time (with DTE)

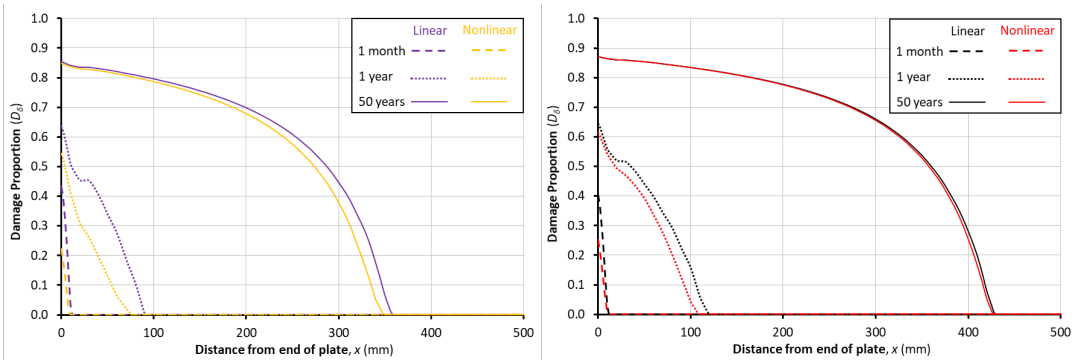

(a) at 30°C (b) at 40°C

Figure 14: Joint damage growth proportion (D_δ) in the strengthened steel beam (with DTE)

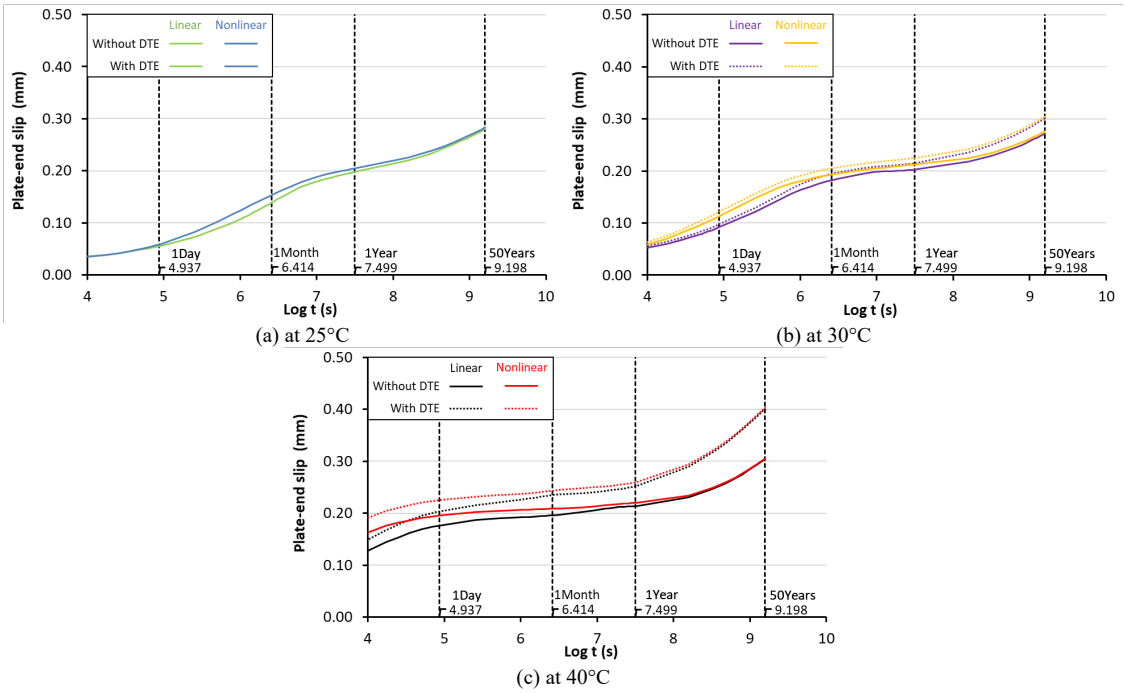

(a) at 25°C (b) at 30°C

(c) at 40°C

Figure 15: Effects of nonlinear and linear creep on the plate-end slip for the different steel beam models

Incorporating nonlinear viscoelasticity has a greater impact on the performance of the CFRP-bonded steel beam at shorter timescales. The difference between the nonlinear and linear plate-end slip is most significant before 1 year. For longer timescales, the linear viscoelastic model is likely to be sufficient. Figure 15 shows, for example, that after 1 day at 40°C (including DTE), the plate-end slip in the nonlinear model is around 10.8% larger than using a linear model. This number dramatically reduces to 4.1% after 1 month, 3.1% after 1 year, and close to 0% after 50 years, which is mainly due to the stress redistribution behaviour resulting in a significant reduction of the stress-dependent nonlinear creep rate.

6 The influence of nonlinear creep on the real-scale FRP-bonded cast-iron beam

The influence of adhesive nonlinear (compared to linear) viscoelasticity on the performance of the FRP-bonded cast-iron structure (Figure 6 (b)) is explored in this section. The CFRP-strengthened cast-iron beam examined is based on a realistic design scenario [1]. It is subjected to a ULS load; however, the brittle nature of cast-iron means that this load demand is relatively low compared to a modern steel beam. Whilst the slip and the CFRP axial stress caused by the external load may be lower, the increased section dimensions can lead to significantly greater DTE behaviour at warm temperatures, which may potentially result in considerable additional slip and CFRP axial stress.

The benchmark results ("no creep") shown in the following figures in this section were obtained from the elastic bond FE analysis, as used in current design guidelines [1,2], and based upon a ULS applied load of 40kN/m [1,31]. The instantaneous maximum shear stress is about 2.3MPa at 25°C, 3.4 MPa at 30°C and 5.2MPa at 40°C with including DTE.

Figure 16 shows the development of the plate-end slip over time at different temperatures, with or without DTE effect (T_{ref} = 25°C). The difference in results between the nonlinear and liner creep is small compared to the DTE effect. The nonlinear slip result is only significantly greater than the results predicted by the linear model at 40°C, including the DTE effect, and this difference diminishes above 1 year.

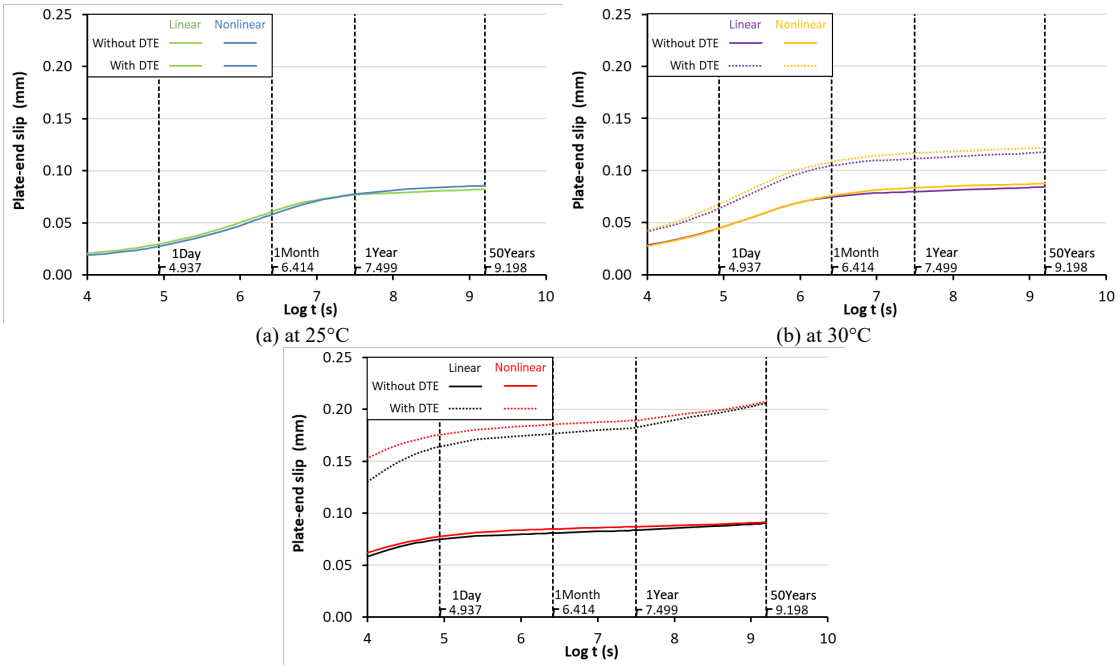

(a) at 25°C (b) at 30°C

(c) at 40°C

Figure 16: Effects of nonlinear and linear creep on the plate-end slip for the different cast-iron beam models

Figure 17 plots the slip distribution along half of the symmetric beam at various sustained temperatures for different time period including DTE. Figure 18 shows the FRP plate tensile stress distribution, also including DTE. The slip distribution in the nonlinear model is larger than that in the linear model; however, this will not result in a significantly lower CFRP stress in the nonlinear model. In the middle of the beam (x = 2000mm), the maximum CFRP stress is larger in the nonlinear model before 1 month at 25°C and 30°C, and thus the effectiveness of strengthening is maintained relatively well during that period by considering the nonlinear viscoelasticity of the adhesive. The damage variable has not been plotted here, as damage did not occur in the joint.

DTE between the CFRP plated and the metallic substrate could make a significant change in the structural behaviour, and DTE might be regarded as enhancing the strengthening by maintaining the CFRP stress during the long-term service. As shown in Figure 18 (c), after 50 years at 40°C as a critical case at warm temperature conditions, the CFRP tensile stress at the *mid-span* of the I-beam is about 60MPa, which is even larger than the initial value at 25°C (noting the different vertical scales). However, this advantage might be lost under cyclic temperature, which is being studied in subsequent research.

7 Comparison of nonlinear and linear creep

The aim of this study has been to compare the effects of nonlinear and linear creep of adhesive on the behaviour of CFRP-bonded metallic structures and to establish whether the nonlinear viscoelastic properties of the adhesive need to be considered, or whether a simpler linear creep model is sufficient.

The numerical analytical work indicates that using a nonlinear rather than a linear viscoelastic constitutive model results in only a slightly larger joint slip (maximum 1.0% after 1 year) and slightly lower CFRP axial stress (maximum 2.4% after 1 year) at short timescales (up to 1 year). The difference between the effects of nonlinear creep and linear creep diminishes at longer timescales, with little difference at 50 years. The joint damage is lower when nonlinear creep is considered, and consequently, this study suggests that using the linear viscoelastic model to analyse the long-term behaviour of an FRP-bonded metallic beam is sufficient for the majority of cases, and it is not necessary to obtain and incorporate a nonlinear viscoelastic constitutive model for the adhesive.

The load and temperature cases applied during the FE analysis of the two beams have been more extreme than would present in a real situation: ultimate limit state loads have been applied and both the load and temperature have been sustained, rather than applying serviceability loads and temperatures that vary with time. However, this does not change the conclusion that a linear creep model will be sufficient for the majority of design cases.

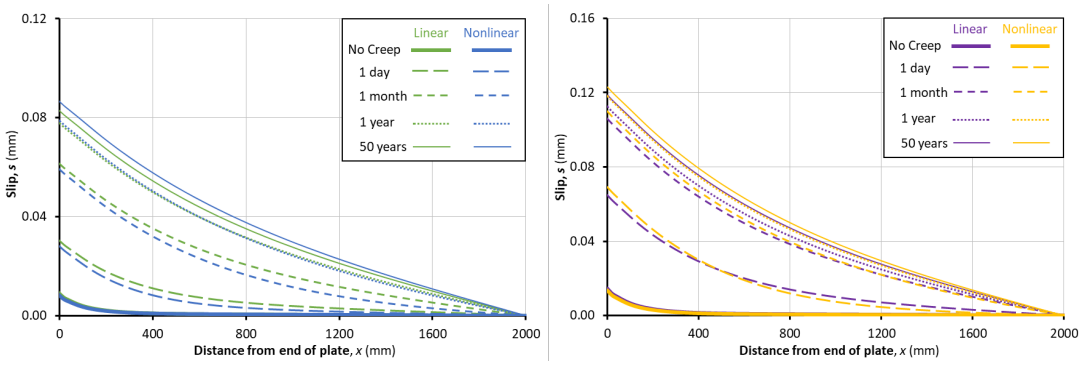

(a) at 25°C (b) at 30°C

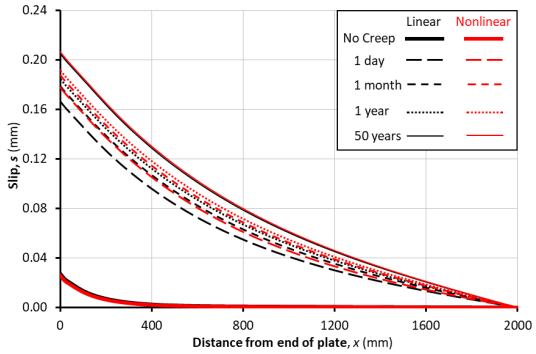

(c) at 40°C

Figure 17: Distribution of joint slip, s (mm) of the strengthened cast-iron beam (with DTE)

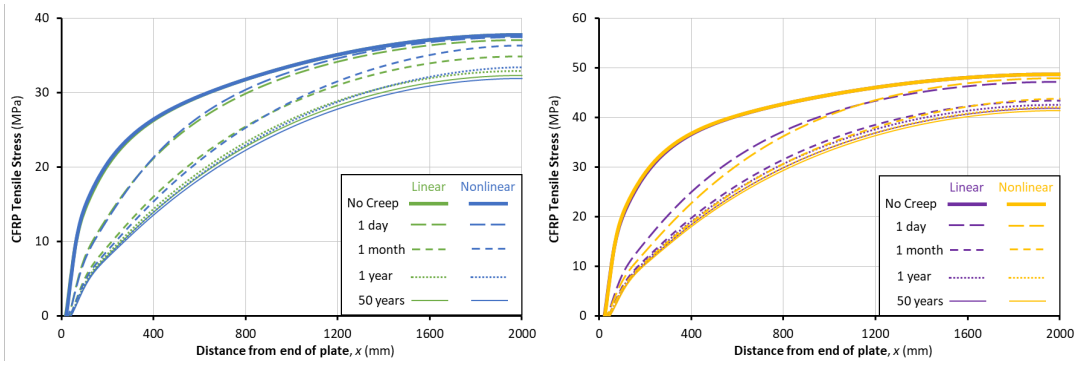

(a) at 25°C (b) at 30°C

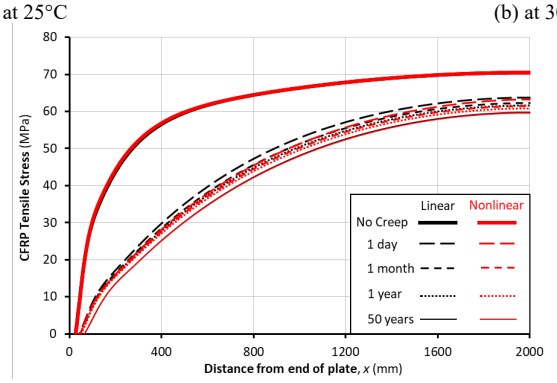

(c) at 40°C

Figure 18: Distribution of FRP tensile stress of the strengthened cast-iron structure with time (with DTE)

At short-term timescales (< 1 year based on the current work), nonlinear viscoelasticity may be necessary if the precise creep behaviour of the strengthened structure is of interest. Nonlinear viscoelasticity could also be significant if a higher temperature or a different type of adhesive is being used that has strong nonlinearity. It would also be significant if the strengthened structure is subjected to higher temperatures; however, it should be noted that the 40°C case considered here is already higher than the maximum operating temperature of (T_g - 15°C) specified in the current design guidance.

8 Conclusions

This paper demonstrates how nonlinear viscoelastic creep affects the behaviour of the CFRP-bonded metallic structures at warm temperatures. The FE studies conducted on two CFRP-strengthened metallic beams compare the relative impact of nonlinear creep and linear creep.

The analytical results of the two examined cases indicate that:

- Characterizing the nonlinear viscoelasticity of the adhesive and implementing it into the FE analyses only leads to a moderately larger joint slip and slightly lower CFRP axial stress during a relatively short period (before 1 year) compared to the linear model. This difference will reduce to almost zero when the time increases to 50 years.
- Considering nonlinear viscoelastic creep will not bring a higher joint damage proportion, and the difference in the maximum FRP stress at the *mid-span* of the beam is minimal, which suggest that the nonlinear creep will not cause more severe structural issues than the linear viscoelastic creep.
- The nonlinear viscoelasticity needs to be considered only when the precise short-term (up to 1 year for the case shown in this paper) nonlinear creep effect is of interest. The simpler linear constitutive model could be utilised reliably to analyse the long-term (longer than 1 year for the case shown in this paper) behaviour of the FRP-bonded metallic beam in most cases.

The difference between the nonlinear creep and linear creep models are smaller for the real-scale cast-iron beam model (which has realistic joint bond stress) compared to the lab-scale steel beam (which has deliberately high joint bond stress). The effect of differential thermal expansion, however, is more significant in the cast-iron structure due to the larger section dimensions. DTE may potentially be beneficial by maintaining the tensile stress in the strengthening FRP plate; however, when the environmental temperature decreases; however, the additional irreversible damage and slip may result in a significant reduction on the effectiveness of FRP-bonded repairing. The present study examines constant elevated temperature and sustained loads that are an extreme case and do not represent the varying temperatures and loads that a real structure will experience. The impact of cyclic temperatures and loads are the subject of a follow-up research; however, this does not affect the conclusion that a linear viscoelastic adhesive model is sufficient for the majority of design cases.

The warm temperature conditions (25°C, 30°C, and 40°C) examined in this paper refer to the environmental temperature that the metallic beam is expected to encounter during normal use, rather than the “high temperature” that may be encountered under direct sunlight. Nevertheless, at the examined temperature conditions, it can already be seen that the effectiveness of strengthening reduces significantly over time. At higher temperature conditions, the speed of this reduction is believed to be even faster, resulting in quicker structural failure.

A major challenge in this research is to characterise the nonlinear viscoelasticity of the structural adhesive at sufficient long timescales at warm temperatures. An accelerated method was applied that combined DMA frequency scans with the TTSP to characteries a commonly used structural adhesive. It should be noted that different types of adhesives (other than Sikadur-330) used in civil engineering could have potentially different nonlinear viscoelastic responses. The conclusions drawn in this study based on characterising the viscoelasticity of Sikadur-330 may not be fully applicable for other types or brands of adhesives. More experimental work may thus be needed to determine their viscoelastic response. Nevertheless, the analyses presented demonstrate the limited difference between the nonlinear creep and linear creep for externally bonding a fibre-reinforced polymer plate for metallic beams.

Data availability

The raw/processed data required to reproduce these findings cannot be shared at this time as the data also forms part of an ongoing study.

CRediT authorship contribution statement

Songbo Wang: Methodology, Formal analysis, Investigation, Writing - original draft, Visualization. **Tim Stratford:** Conceptualization, Resources, Writing - review & editing, Supervision. **Thomas P S Reynolds:** Writing - review & editing, Supervision.

Declaration of competing interest

The authors declare that they have no known competing financial interests or personal relationships that could have appeared to influence the work reported in this paper.

Acknowledgments

This research did not receive any specific grant from funding agencies in the public, commercial, or not-for-profit section.

References

[1] Cadei JMC, Stratford TJ, Hollaway LC, Duckett WG. Strengthening metallic structures using externally bonded fibre-reinforced polymers, Construction Industry Research and Information Association (CIRIA), London, UK, 2004.

[2] National Research Council Advisory Committee. Guidelines for the design and construction of externally bonded FRP systems for strengthening existing structures - metallic structures., Rome, Italy: National Research Council ; 2007.

[3] Darby A, Ibell T, Clarke J. TR55 Design guidance for strengthening concrete structures using fibre composite materials, The Concrete Society, Surrey, UK, 2004.

[4] American Concrete Institute (ACI), Aci 440.2R-08: Guide for the design and construction of externally bonded FRP systems for strengthening concrete structures, USA, 2008.

[5] Zhao X-L. FRP-strengthened metallic structures, Taylor and Francis, Boca Rotan, FL, 2013.

[6] Wang S, Stratford T, Reynolds T. Creep of Adhesively-bonded FRP-strengthened Steel Structures at Elevated Temperatures, in Proceedings of the 9th Biennial Conference on Advanced Composites in Construction (ACIC2019)., Birmingham, UK, 2019.

[7] Ascione F, Granata L, Lombardi A. The influence of the hygrothermal aging on the strength and stiffness of adhesives used for civil engineering applications with pultruded profiles: an experimental and numerical investigation. J Adhes 2021;00:1–39. https://doi.org/10.1080/00218464.2021.1936507.

[8] Ascione F, Granata L, Guadagno L, Naddeo C. Hygrothermal durability of epoxy adhesives used in civil structural applications. Compos Struct 2021;265:113591. https://doi.org/10.1016/j.compstruct.2021.113591.

[9] Stratford TJ, Bisby LA. Effect of warm temperatures on externally bonded FRP strengthening. J Compos Constr 2012;16:235–44. https://doi.org/10.1061/(ASCE)CC.1943-5614.0000260.

[10] Sahin MU, Dawood M. Experimental Investigation of Bond between High-Modulus CFRP and Steel at Moderately Elevated Temperatures. J Compos Constr 2016;20:1–11. https://doi.org/10.1061/(ASCE)CC.1943-5614.0000702.

[11] Zhang C, Wang J. Viscoelastic analysis of FRP strengthened reinforced concrete beams. Compos Struct 2011;93:3200–8. https://doi.org/10.1016/j.compstruct.2011.06.006.

[12] Jeong Y, Lopez MM, Bakis CE. Effects of temperature and sustained loading on the mechanical response of CFRP bonded to concrete. Constr Build Mater 2016;124:442–52. https://doi.org/10.1016/j.conbuildmat.2016.07.123.

[13] Emara M, Torres L, Baena M, Barris C, Moawad M. Effect of sustained loading and environmental conditions on the creep behavior of an epoxy adhesive for concrete structures strengthened with CFRP laminates. Compos Part B Eng 2017;129:88–96. https://doi.org/10.1016/j.compositesb.2017.07.026.

[14] Wang S, Stratford T, Reynolds TPS. Linear creep of bonded FRP-strengthened metallic structures at warm service temperatures. Constr Build Mater 2021;283:122699. https://doi.org/10.1016/j.conbuildmat.2021.122699.

[15] Findley WN, Lai JS, Onaran K. Creep and Relaxation of Nonlinear Viscoelastic Materials with an introduction to linear viscoelasticity, North-Holland Publishing Company, Amsterdam, 1989.

[16] Majda P, Skrodzewicz J. A modified creep model of epoxy adhesive at ambient temperature. Int J Adhes Adhes 2009;29:396–404. https://doi.org/10.1016/j.ijadhadh.2008.07.010.

[17] Houhou N, Benzarti K, Quiertant M, Chataigner S, Fléty A, Marty C. Analysis of the nonlinear creep behavior of concrete/FRP-bonded assemblies. J Adhes Sci Technol 2014;28:1345–66. https://doi.org/10.1080/01694243.2012.697387.

[18] Wang S, Stratford T, Reynolds T. Nonlinear creep of the adhesive bond in FRP-strengthened steel beams, in Proceedings of the Seventh Asia-Pacific Conference on FRP in Structures (APFIS 2019), Surfers Paradise, Gold Coast, Austrilia, 2019.

[19] Ropers S, Sachs U, Kardos M, Osswald TA. A thermo-viscoelastic approach for the characterization and modeling of the bending behavior of thermoplastic composites – Part II. Compos Part A Appl Sci Manuf 2017;96:67–76.

https://doi.org/10.1016/j.compositesa.2017.02.007.
[20] Aldhufairi HS, Olatunbosun O, Essa K. Determination of a Tyre's Rolling Resistance Using Parallel Rheological Framework. SAE Tech Pap 2019;2019-Janua:1–11. https://doi.org/10.4271/2019-01-5069.
[21] Abouhamzeh M, Sinke J, Jansen KMB, Benedictus R. Kinetic and thermo-viscoelastic characterisation of the epoxy adhesive in GLARE. Compos Struct 2015;124:19–28. https://doi.org/10.1016/j.compstruct.2014.12.069.
[22] Hurtado J, Lapczyk I, Govindarajan S. Parallel rheological framework to model non-linear viscoelasticity, permanent set, and Mullins effect in elastomers. Const Model Rubber 2013;8:95–100.
[23] Abaqus. ABAQUS user's manual 6.14., ABAQUS Inc, 2014
[24] Rackl M. Curve fitting for Ogden, Yeoh and polynomial models. in Proceedings of ScilabTEC Conference, Regensburg, 2015.
[25] Menard KP. Dynamic Mechanical Analysis: A Practical Introduction, Second Edition, Taylor and Francis, Boca Rotan, FL, 2008.
[26] Guedes RM. Creep and fatigue in polymer matrix composites, Woodhead Publishing Limited, Camcridge, UK, 2011. https://doi.org/10.1016/C2017-0-02292-9.
[27] SIKA, Sikadur®-330 Data Sheet, Sika Construction Chemicals, 2017.
[28] PerkinElmer Inc., DMA8000 Help Files, n.d.
[29] International Organization for Standardization. Plastics — Determination of dynamic mechanical properties, ISO 6721:2019, Geneva, Switzerland, 2019.
[30] Othman D, Stratford T, Bisby L. A Comparison of On-Site and Elevated Temperature Cure of an FRP Strengthening Adhesive, in Proceedings of Fibre Reinforced Polymer Reinforced Concrete Structures (FRPRCS11), Guimarães, Portugal, 2013.
[31] Stratford T, Cadei J. Elastic analysis of adhesion stresses for the design of a strengthening plate bonded to a beam. Constr Build Mater 2006;20:34–45. https://doi.org/10.1016/j.conbuildmat.2005.06.041.
[32] M Emerson. Forth Road Bridge : temperature measurements, Transport Research Laboratory (TRL REPORT) 472, Berkshire, UK, 2000.
[33] Highways Agency. Design manual for roads and bridges., London, UK: HM Stationery Office; 1994.
[34] Zhou H, Torres JP, Fernando D, Law A, Emberley R. The bond behaviour of CFRP-to-steel bonded joints with varying bond properties at elevated temperatures. Eng Struct 2019;183:1121–33. https://doi.org/10.1016/j.engstruct.2018.10.044.
[35] Xia SH, Teng JG. Behaviour of FRP-to-steel bonded joints, in Proceedings of Internatioal Symposiumon Bond Behaviour of FRP in Structures (BBFS 2005), Hong Kong, China, 2005.
[36] De Lorenzis L, Zavarise G. Cohesive zone modeling of interfacial stresses in plated beams. Int J Solids Struct 2009;46:4181–91. https://doi.org/10.1016/j.ijsolstr.2009.08.010.